

New approach to initializing hydrodynamic fields and mini-jet propagation in quark-gluon fluids

Michito Okai,^{1,*} Koji Kawaguchi,^{1,†} Yasuki Tachibana,^{2,1,‡} and Tetsufumi Hirano^{1,§}

¹*Department of Physics, Sophia University, Tokyo 102-8554, Japan*

²*Institute of Particle Physics and Key Laboratory of Quark and Lepton Physics (MOE), Central China Normal University, Wuhan, 430079, China*

(Dated: November 5, 2018)

We propose a new approach to initialize the hydrodynamic fields such as energy density distributions and four flow velocity fields in hydrodynamic modeling of high-energy nuclear collisions at the collider energies. Instead of matching the energy-momentum tensor or putting the initial conditions of quark-gluon fluids at a fixed initial time, we utilize a framework of relativistic hydrodynamic equations with source terms to describe the initial stage. Putting the energy and momentum loss rate of the initial partons into the source terms, we obtain hydrodynamic initial conditions dynamically. The resultant initial profile of the quark-gluon fluid looks highly bumpy as seen in the conventional event-by-event initial conditions. In addition, initial random flow velocity fields also are generated as a consequence of momentum deposition from the initial partons. We regard the partons that survive after the dynamical initialization process as the mini-jets and find sizable effects of both mini-jet propagation in the quark-gluon fluids and initial random transverse flow on the final momentum spectra and anisotropic flow observables. We perform event-by-event (3 + 1)-dimensional ideal hydrodynamic simulations with this new framework that enables us to describe the hydrodynamic bulk collectivity, parton energy loss, and interplay among them in a unified manner.

PACS numbers: 25.75.-q, 12.38.Mh, 25.75.Ld, 24.10.Nz

I. INTRODUCTION

High-energy nuclear collision experiments are performed at the Large Hadron Collider (LHC) at CERN and at the Relativistic Heavy Ion Collider (RHIC) at Brookhaven National Laboratory (BNL) towards the understanding of bulk and transport properties of the deconfined nuclear matter, the quark gluon plasma (QGP) [1]. One of the major discoveries at the RHIC is large azimuthal anisotropy [2–11], which is comparable with the results from relativistic hydrodynamic models [12–16]. This triggers a lot of further theoretical and experimental efforts to deeply understand the QGP fluids.

Hydrodynamic modelings have been greatly developed as the most standard approach to describe the soft dynamics in high-energy nuclear collisions [17–27]. Especially, one of the most advanced models is to combine fully (3+1)-dimensional dissipative hydrodynamics with some initialization models and hadronic cascade codes so that one describes the whole stage from event-by-event initial hydrodynamic states to a final hadronic afterburner [28–32]. This model enables one to extract transport properties of the QGP fluids from a variety of experimental data. However how the system reaches local thermal equilibrium rapidly after the first contact, which is suggested from the success of hydrodynamic modeling, is not well understood yet. This is a longstanding open

problem and its solution is highly demanded.

Although the hybrid type model mentioned above has been successful in the description of the bulk dynamics in high-energy nuclear collisions, the model is applicable only in the soft sector, i.e., in the low transverse momentum (p_T) regions. On the other hand, hard partons are produced together with the QGP at the collider energies and are subject to lose their energy and momentum as they traverse the bulk medium. To quantify the amount of energy loss in the dynamically evolving QGP, realistic solutions of relativistic hydrodynamic equations are utilized in Refs. [33–35]. These studies aimed at describing hydrodynamic bulk collectivity in the low- p_T regions and jet quenching in the high- p_T regions at once. At that time, the lost energies are so small that these are not expected to change the bulk dynamics dramatically. Later the contribution of the medium response to the jet propagation has been focused in the studies of jet substructure and recognized to be very important [36–39]. In particular, very recently, it turns out that enhancement of yields observed at the large angles from the jet axis [40] is interpreted quantitatively from hydrodynamic responses to the jet propagation [41]. This suggests that the interplay between soft collective dynamics and hard jet propagation becomes more and more important.

In addition to the jets with $p_T \gtrsim 100$ GeV, a large number of mini-jets with $p_T \sim 2$ -10 GeV also are produced, in particular, at the LHC energies. With this line of thought, there is a very first attempt to include propagation of *multiple* mini-jets in the QGP fluids and to study its consequences in flow observables [42]. In Ref. [42], the optical Glauber model is employed for the initialization of hydrodynamic fields, and the resultant initial en-

* michito0605@eagle.sophia.ac.jp

† kawaguchi@eagle.sophia.ac.jp

‡ yasuki.tachibana@mail.ccnu.edu.cn

§ hirano@sophia.ac.jp

ergy density distributions are smooth functions.¹ This means that the higher order anisotropy v_n ($n > 3$) is induced mainly by the disturbance of the QGP fluids due to mini-jet propagation. Although one is able to directly extract the effect of mini-jet propagation on flow observables, there must be a complicated interplay among various mechanisms which generate azimuthal anisotropy. These should be non-linear effects that the final v_n is not the sum of all possible effects. One dominant mechanism of generating azimuthal anisotropy should be fluctuating initial profiles from event to event. Since the origin of mini-jets and that of hot spots of the medium in fluctuating initial profiles are the same, i.e., nucleon-nucleon inelastic collisions at the first contact of two nuclei, it is not obvious to divide soft (the medium) from hard (the mini-jets) components. This, in turn, demands a framework to treat soft and hard components at once, both in the initial states and during the evolution of the system. Thus, the main purpose of this paper is to develop the first dynamical model to do so within hydrodynamic modeling. As an application of this model, we investigate the effects of mini-jet propagation on transverse-momentum spectra and anisotropic flow in Pb+Pb collisions at the LHC energy.

The paper is organized as follows. In Sec. II, we explain a new approach to generate hydrodynamic fields. We show results of transverse momentum spectra, elliptic flow, and triangular flow coefficients in Pb+Pb collisions at the LHC energy in Sec. III. Section IV is devoted to a summary of the paper.

We use the natural unit, $\hbar = c = k_B = 1$, and the Minkowski metric, $g^{\mu\nu} = \text{diag}(1, -1, -1, -1)$, throughout this paper.

II. MODEL

We formulate a model in which all the matters produced in high-energy nuclear collisions are supposed to arise from the partons created at the first contact of two nuclei. We generate the partons by estimating their production from an event generator PYTHIA [43] combined with the Monte Carlo version of the Glauber model (MC-Glauber) [44]. Then, these partons start to travel through the vacuum after their production and are assumed to lose their energy and momentum until either the preassigned hydrodynamic initial time or the time when their energies vanish completely. In the meantime, all the lost energy and momentum are put into the source term of hydrodynamic equations to generate medium fluids gradually. After the hydrodynamic initial time, the

dynamics is the same as a conventional QGP fluid + jet approach [36, 41, 45]: Surviving partons are regarded as mini-jets and deposit their energy and momentum while traversing the fluids until their energies vanish completely or they escape from the fluids. The fluid evolves under the influence of the mini-jet propagation according to the hydrodynamic equations with source terms. Finally, the particle spectra from the fluids are calculated via the Cooper-Frye formula [46].

A. Distribution of partons in phase space

We first use the MC-Glauber model to estimate the number of participants and that of binary collisions at some transverse point \mathbf{x}_\perp . For each pair of binary collisions, we run PYTHIA for one inelastic $p+p$ collision with switching off fragmentation. Note that we neglect possible iso-spin effects in the initial collisions.

An incoherent sum of PYTHIA results for pairs of all binary collisions would mean that multiplicity scales with N_{coll} . However, N_{coll} scaling is anticipated only in high- p_T regions. On the other hand, the dominant source of multiplicity is soft, namely, low- p_T particles. To account for approximate N_{part} scaling of multiplicity, and to demonstrate the idea of a “rapidity triangle or trapezoid” [47–50], one needs to perform a rejection sampling from the particle ensemble in PYTHIA².

From the MC-Glauber model, we first pick up two nucleons (say, A and B , respectively) undergoing a binary collision. Transverse positions of nucleon A (positive beam rapidity) and nucleon B (negative beam rapidity) are assumed to be $\mathbf{x}_{\perp,A}$ and $\mathbf{x}_{\perp,B}$, respectively. We next count the number of binary collisions for each nucleon: N_A (N_B) means the number of nucleons which are collided by nucleon A (B). Then we perform a rejection sampling for partons with transverse-momentum $p_T = \sqrt{p_x^2 + p_y^2}$ and rapidity $Y = (1/2) \ln[(E + p_z)/(E - p_z)]$ from PYTHIA with a momentum-dependent acceptance function,

$$w(p_T, Y) = w(Y) \times \frac{1}{2} \left[1 - \tanh \left(\frac{p_T - p_{T0}}{\Delta p_T} \right) \right] + 1 \times \frac{1}{2} \left[1 + \tanh \left(\frac{p_T - p_{T0}}{\Delta p_T} \right) \right], \quad (1)$$

$$w(Y) = \frac{Y_b + Y}{2Y_b} \frac{1}{N_A} + \frac{Y_b - Y}{2Y_b} \frac{1}{N_B}. \quad (2)$$

¹ The authors of Ref. [42] investigated the “hot spot” scenario in which hard partons instantaneously deposit their energy to create a hot spot on top of a smooth background. However, this is different from what we address in the following sections since the profile of the background medium also fluctuates.

² Hydrodynamic initial conditions which contain the idea of a “rapidity triangle or trapezoid” have been extensively discussed in Refs. [49, 50]. In these studies, rapidity distributions in $p+p$ collisions were parametrized simply by using a smooth function. Whereas, in the present paper, we employ PYTHIA for particle production. Multiplicity and the longitudinal profile fluctuate in this model, which is important, especially, in small colliding systems [51].

Here Y_b is the beam rapidity, p_{T0} is a parameter to divide soft and hard transverse-momentum regions, and Δp_T is a width parameter for the crossover region. We repeat this procedure for each pair of nucleons undergoing a binary collision in one heavy-ion collision event. Notice that the case of $N_A = N_B = 1$ results in an ordinary single PYTHIA event.

Let us suppose N_A nucleons (with *negative* beam rapidity) and N_B nucleons (with *positive* beam rapidity) are collided with each other. It should be noted that N_A means the number of nucleons collided by nucleon A which is going with *positive* beam rapidity. In this case, the number of binary collisions is given by $N_{\text{coll}} = N_A N_B$ and we call $N_A N_B$ times inelastic $p+p$ events from PYTHIA. Then for each two-dimensional bin of p_T and Y in each binary collision, we take samples of the partons by using the acceptance function (1). In the high- p_T region, the parton yields scale with

$$N_A N_B w(p_T \gg p_{T0}, Y) \approx N_A N_B \equiv N_{\text{coll}}. \quad (3)$$

Therefore, all the partons created in $N_A N_B$ times PYTHIA simulations remain at the high- p_T limit in the entire rapidity region even after the rejection. Whereas, in the low- p_T region, the parton multiplicity scales with

$$\begin{aligned} N_A N_B w(p_T \ll p_{T0}, Y) &\approx N_A N_B w(Y) \\ &= \frac{Y_b + Y}{2Y_b} N_B + \frac{Y_b - Y}{2Y_b} N_A. \end{aligned} \quad (4)$$

Thus, at the low- p_T limit, the number of partons remaining after the rejection exhibits rapidity distributions under the idea of a rapidity triangle or trapezoid: The parton yields at beam rapidity $Y = Y_b(-Y_b)$ after the rejection reduce to those obtained from N_B (N_A) times PYTHIA simulations. At midrapidity $Y = 0$, the multiplicity scales with

$$N_A N_B w(p_T \ll p_{T0}, Y = 0) \approx \frac{N_A + N_B}{2} \equiv \frac{N_{\text{part}}}{2} \quad (5)$$

as anticipated.

Figure 1 shows a p_T distribution of initial partons in one central ($b = 0$ fm) Pb+Pb event at $\sqrt{s_{NN}} = 2.76$ TeV. Here we choose parameters $p_{T0} = 2$ GeV and $\Delta p_T = 1$ GeV. These parameters should have been determined through comparison of the model results with, e.g., experimental data of nuclear modification factors R_{AA} . However, such detailed but time-consuming analyses will be postponed for future work. Hence we fix these parameters so as to obtain a smooth p_T distribution in this paper.

Using transverse positions of the pair of binary collision and rapidity of a produced parton, positions of the produced parton i in the configuration space are determined to be

$$\mathbf{x}_{\perp}^i = (x^i, y^i) = \frac{\mathbf{x}_{\perp,A} + \mathbf{x}_{\perp,B}}{2} + \frac{\mathbf{x}_{\perp,A} - \mathbf{x}_{\perp,B}}{2Y_b} Y^i, \quad (6)$$

$$\eta_s^i = Y^i. \quad (7)$$

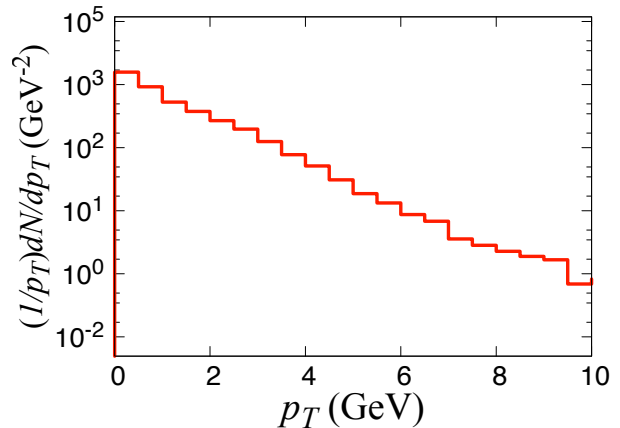


FIG. 1. (Color online) The p_T spectrum of the initial partons in one central ($b = 0$ fm) Pb+Pb collision at $\sqrt{s_{NN}} = 2.76$ TeV. The number of binary collisions is estimated to be $N_{\text{coll}} = 1983$ in this particular event.

Thus the positions in the configuration space are determined mainly from the MC-Glauber model. Transverse positions (6) slightly are shifted randomly within the geometrical cross section in inelastic $p+p$ collisions, σ_{in}^{pp} . Here we implicitly assume that particle production occurs in the transverse area of a hadron string or a color flux tube which is elongated along Eq. (6) in rapidity space.

In this way, we obtain phase-space distributions of partons just after collisions of high-energy nuclei $f(t = 0^+, \mathbf{x}; \mathbf{p})$ on an event-by-event basis.

B. Hydrodynamic equations with source terms

Relativistic hydrodynamic equations with source terms

$$\partial_{\mu} T^{\mu\nu} = J^{\nu} \quad (8)$$

have been used extensively in the physics of jet quenching and its effects on medium [36, 41, 45]. Here $T^{\mu\nu}$ is the energy-momentum tensor of the fluids, and J^{ν} is the source term for the fluids. In this paper, we neglect possible dissipative effects, which brings the energy-momentum tensor to be $T^{\mu\nu} = (e + P)u^{\mu\nu} - Pg^{\mu\nu}$, where e is the energy density, P is the pressure, and u^{μ} is the four-fluid velocity. We employ an equation of state from a recent lattice QCD result [52]. Here it is assumed that energy and momentum deposited from partons are instantaneously equilibrated. We utilize this framework to generate initial hydrodynamic fields dynamically.

We introduce two time scales, τ_{00} and τ_0 . At $\tau = \sqrt{t^2 - z^2} = 0$ fm, the highly Lorentz-contracted two nuclei are collided with each other at $z = 0$ fm and partons are produced as discussed in the previous subsection. Until τ_{00} , all partons are supposed to be formed. Thus τ_{00}

can be regarded as the formation time of the partons. From τ_{00} to τ_0 , all partons travel while losing their energy and momentum regardless of whether the medium exists at the position of the partons. To do so, we solve Eq. (8) with vanishing initial conditions of hydrodynamic fields $T^{\mu\nu}(\tau = \tau_{00}) = 0$ until τ_0 by modeling the source terms:

$$J^\mu(x) = \sum_i J_i^\mu(x), \quad (9)$$

$$J_i^\mu(x) = -\frac{dp_i^\mu}{dt} \delta^{(3)}(\mathbf{x} - \mathbf{x}_i(p_i, t)), \quad (10)$$

$$\mathbf{x}_i(t) = \mathbf{x}_i(t=0) + \frac{\mathbf{p}_i}{p_i^0} t. \quad (11)$$

Here the summation is taken over all partons. In this paper, we assume a constant energy and momentum loss rate of $dE_i/dt = d|\mathbf{p}_i|/dt = 5$ GeV/fm at $\tau_{00} < \tau < \tau_0$. We solve hydrodynamic equations with source terms (8) until $\tau = \tau_0$ to obtain hydrodynamic initial states in the ordinary sense.

In the analysis of the observables, we have an option that all four fluid velocities are reset to be the Bjorken scaling solution [53] at $\tau = \tau_0$. This option mimics a conventional event-by-event Glauber-type initial condition which has a bumpy profile of matter density and no transverse flow on the transverse plane.

C. Freeze-out and flow coefficients

After $\tau = \tau_0$, we continue to solve Eq. (8) until the maximum temperature goes below a fixed decoupling temperature of $T = T_{\text{dec}}$. The energy loss of the mini-jets in the QGP fluids after $\tau = \tau_0$ will be discussed in the next subsection. To obtain the momentum distributions of hadrons from the medium after the hydrodynamic evolution, we use the Cooper-Frye formula [46],

$$E \frac{dN_i}{d^3p} = \frac{g_i}{(2\pi)^3} \int_{\Sigma} \frac{p^\mu d\sigma_\mu(x)}{\exp[p^\mu u_\mu(x)/T(x)] \mp_{\text{BF}} 1}, \quad (12)$$

where g_i is the degeneracy, \mp_{BF} corresponds to Bose or Fermi statistics for hadron species i , and Σ is the freeze-out hypersurface. Here the freeze-out is assumed to occur at a fixed temperature of $T_{\text{dec}} = 160$ MeV.

Flow coefficients of azimuthal angle distributions at midrapidity $Y = 0$, are calculated from the event plane method. The event plane angle of the n -th order for the j -th event is obtained as

$$\tan n\Psi_n^j = \frac{\langle \sin n\phi_p \rangle_j}{\langle \cos n\phi_p \rangle_j}, \quad (13)$$

where ϕ_p is the azimuthal angle in the momentum space and the angle bracket means the average over the particle ensemble at midrapidity $Y = 0$ in a single event,

$$\langle \mathcal{O} \rangle_j = \frac{\int dp_T d\phi_p \mathcal{O} \frac{dN^j}{dp_T d\phi_p dY}}{\int dp_T d\phi_p \frac{dN^j}{dp_T d\phi_p dY}} \Bigg|_{Y=0}. \quad (14)$$

Averaging over all events, we obtain the flow coefficients as a function of p_T at midrapidity $Y = 0$,

$$v_n(p_T) = \frac{1}{N_{\text{ev}}} \sum_j \frac{\int d\phi_p \cos n(\phi_p - \Psi_n^j) \frac{dN^j}{dp_T d\phi_p dY}}{\int d\phi_p \frac{dN^j}{dp_T d\phi_p dY}} \Bigg|_{Y=0}. \quad (15)$$

In this paper, we calculate spectra and flow coefficients of charged pions directly emitted from the decoupling hypersurface. For more quantitative analyses, the effects of hadronic rescatterings on and the contribution of the decays of hadron resonances and that of fragmentation of mini-jets to final spectra and flow coefficients are necessary to be taken into account. We would like to leave them for a future study.

D. Energy loss of mini-jets

From $\tau = \tau_0$, we treat the surviving partons as mini-jets propagating through the medium. The mini-jets deposit their energy and momentum into the QGP fluid. We use the energy-loss rate for the mini-jets of the form [54]:

$$\frac{dE_i}{dt} = - \left[\frac{T(t, \mathbf{x}_i(t))}{T_0} \right]^3 \frac{dE}{dt} \Bigg|_0, \quad (16)$$

where T_0 and $dE/dt|_0$ are the reference temperature and the reference energy-loss rate, respectively. In this paper, $T_0 = 500$ MeV and $dE/dt|_0 = 5$ GeV/fm are chosen to give the typical values of the nuclear modification factor for high- p_T particles ($p_T \sim 10$ GeV/ c) in central Pb+Pb collisions at the LHC [55, 56]. The mini-jets continue to deposit their energy into the QGP medium according to Eq. (16) until the local temperature drops to $T_{\text{dec}} = 160$ MeV or until their energy vanishes. We assume that the mini-jet partons are massless and lose their momenta together with energy as

$$\frac{d\mathbf{p}_i}{dt} = \frac{\mathbf{p}_i}{|\mathbf{p}_i|} \frac{dE_i}{dt}. \quad (17)$$

E. Remarks

One is able to treat soft and hard physics in a unified manner in this model in principle. At the moment, the model for the particle production and four-momentum loss are quite simple. Although our dynamical initialization process would capture some aspects of local thermalization, we admit this would not be the actual thermalization process. Nevertheless, our approach could be a first step toward constructing a unified framework in full phase space based on relativistic hydrodynamics. In the near future, we will estimate final hadrons from mini-jets that survived in the final state via fragmentation. Thus we obtain the resulting spectra in the entire momentum region in high-energy nuclear collisions, starting from the

partons created at the very initial stage. Since soft and hard particles are treated at once, correlations between soft and hard physics are naturally encoded in the framework.

In the conventional Glauber-model-based initialization, energy and momentum are not conserved when hydrodynamic fields are set. The thermodynamic entropy density distribution of the medium is estimated from the number of participants, binary collisions, or produced particles. In this process, one often introduces an adjusting parameter of the multiplicity, or replaces particles with Gaussian functions with some smearing parameters. Also, initial flow velocity is often chosen from the Bjorken scaling solution [53] and is assumed to vanish in the transverse direction. In this case, the energy-momentum tensor does not match before and after initialization.³ On the other hand, energy and momentum are conserved in the present framework all the way through dynamical initialization. There is no concept of matching the energy-momentum tensor between pre-equilibrium physics and hydrodynamics at the hydrodynamic initial time τ_0 , no room for adjusting overall normalization of multiplicity, or no smearing parameters from particles to hydrodynamic fields in this model. At $\tau = \tau_0$, the initial flow appears as a consequence of momentum deposition from initial partons. Hence one does not need to parametrize the initial flow. Note that the total energy is not exactly the same as the collision energy in the current setting since we just combine the MC-Glauber model with PYTHIA. In particular, the concept of N_{coll} implies the same N_{coll} times $p+p$ collisions at $\sqrt{s_{NN}}$ happen, which obviously overestimates the total energy of a collision. This could be resolved in principle by employing more sophisticated event generators. At present, our aim is to construct a framework of a unified approach in the entire phase space based on the Glauber picture. Therefore, the results obtained in this paper should give a baseline of the follow-up studies.

III. RESULTS

A. Initial states

In the actual analysis, we choose $\tau_{00} = 0.1$ and $\tau_0 = 0.6$ fm throughout this paper. Figure 2 shows snapshots of the medium energy density distributions (left panels) and those of the transverse flow velocity distributions (right panels) in a Pb+Pb collision at the LHC energy during

³ Given the fact that a complete pre-thermalization model does not exist, the system is still far away from the local equilibrium state at the matching. In this case, the dissipative correction to an ideal part of energy-momentum tensor, $\delta T^{\mu\nu} = T^{\mu\nu} - T_{\text{ideal}}^{\mu\nu}$, must be huge so that dissipative hydrodynamics cannot be applicable.

the dynamically generating process of the initial hydrodynamic fields. In these examples, the impact parameter is chosen to vanish for illustrative purposes. The snapshots are taken on the transverse plane at $\eta_s = 0$ at $\tau = 0.15, 0.4,$ and 0.6 fm. We see the gradual growth of the relatively higher-energy density area. As partons lose their energies while traveling in vacuum or a medium, the medium energy density tries to increase rapidly. On the other hand, the volume of the system expands in the longitudinal direction, which would reduce the medium energy density on the transverse plane. As a consequence, there is a competition between the growth and the dilution of the medium energy density during dynamical initialization. For a fluid element at the fixed transverse position, some partons come in during dynamical initialization and deposit their energy. Thus energy density at that point suddenly increases. The energy density can decrease as the “hot spot” expands radially. Thus the time evolution of the energy density is a consequence of these various effects. To see this more clearly, we show the time evolution of the energy density at some fixed transverse positions in Fig. 3.

The energy density profiles in the left panels of Fig. 2 look highly bumpy and quite similar to the conventional event-by-event initial conditions using the MC-Glauber model. However, a major difference between the present approach and the conventional MC-Glauber type initialization is, as shown in the right panels of Fig. 2, the appearance of random transverse flow at $\tau = \tau_0$ which originates from random directions of the partons generated at the first contact.

Figure 4 shows the p_T spectra of the partons before and after dynamical initialization in 30-40% Pb+Pb collisions at $\sqrt{s_{NN}} = 2.76$ TeV. Hereafter the color bands in the figures represent the statistical errors. Here we fix an impact parameter of $b = 9.32$ fm, and the number of events is $N_{\text{ev}} = 10^2$. It should be noted that a peak at the lowest- p_T bin in the results at $\tau = \tau_0$ contains partons with vanishing energy and momentum. These surviving partons at $\tau = \tau_0$ traverse the medium as mini-jets.

B. Spectra and flow

In Fig. 5, the p_T spectra of charged pions at midrapidity in the four settings are compared with each other. Here we average over $N_{\text{ev}} = 10^2$ times Pb+Pb events at $b = 10.58$ fm. The p_T spectrum looks like power-law behavior in our default setting [$\Delta E \neq 0, v_T(\tau_0) \neq 0$] in which random transverse flow appears at $\tau = \tau_0$ and, subsequently, the surviving partons traverse the QGP medium as depositing their energy and momentum. The p_T spectrum is quite similar to the case when energy and momentum losses are switched off after $\tau = \tau_0$ [$\Delta E = 0, v_T(\tau_0) \neq 0$]. The effect of mini-jet propagation is not significant in the p_T spectra when the initial velocity is induced during the dynamical generation of the hydrodynamic fields. On the other hand, an exponential decrease

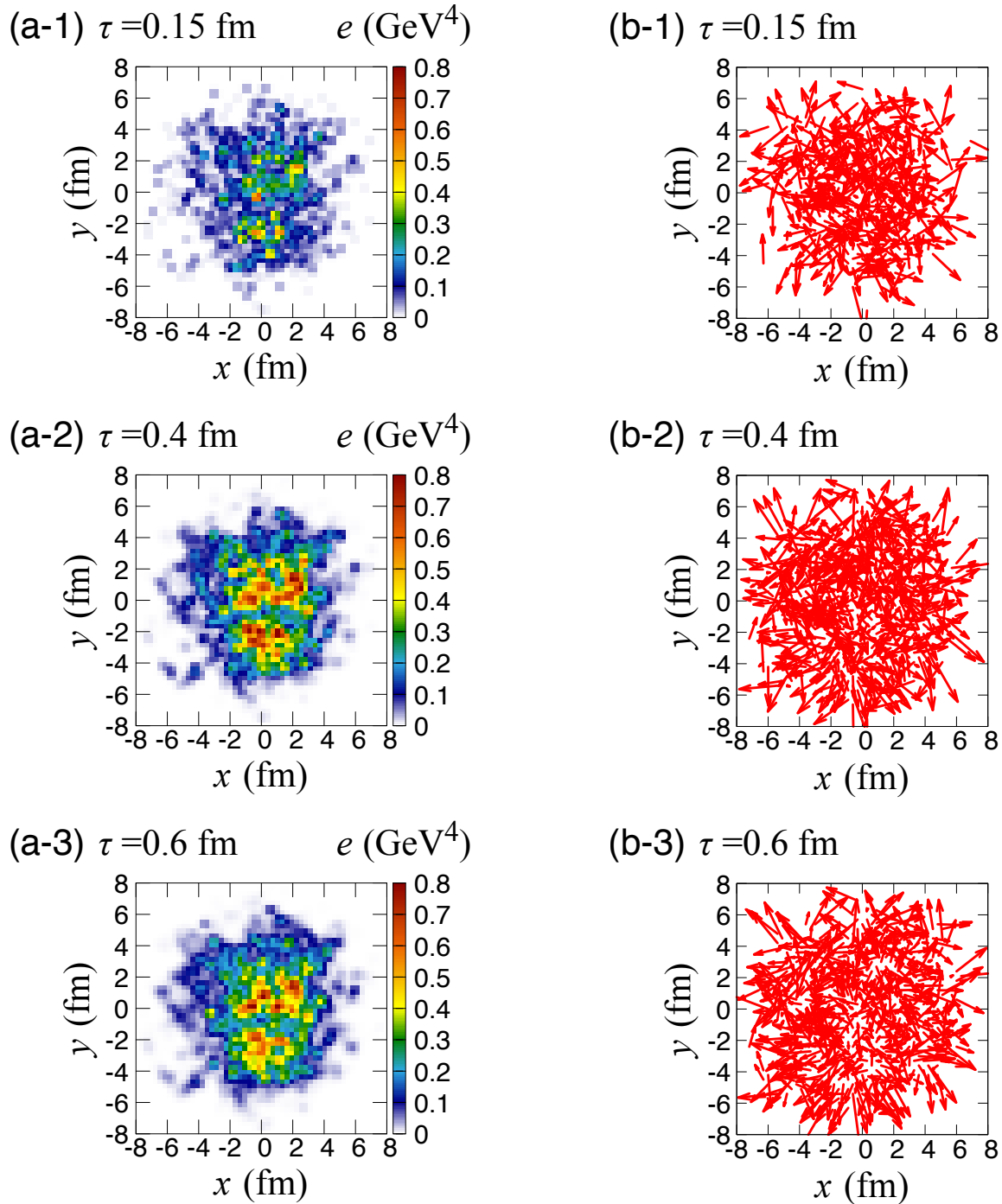


FIG. 2. (Color online) Snapshots of the medium energy density distribution in units of GeV^4 (left panels) and the transverse flow velocity (right panels), on the transverse plane in a Pb+Pb collision at the LHC energy. From top to bottom, $\tau = 0.15$, 0.4, and 0.6 fm, respectively. The impact parameter is $b = 0.0$ fm for illustrative purposes.

with increasing p_T is seen when transverse flow velocity is forced to vanish at $\tau = \tau_0$ [$\Delta E = 0$, $v_T(\tau_0) = 0$], which is consistent with the result from hydrodynamic models with the conventional Glauber-type initial conditions. As a consequence, the yields above $p_T \sim 3$ GeV

in these cases are much smaller than the ones with initial transverse flow. This is the case even when mini-jets lose energy and momentum [$\Delta E \neq 0$, $v_T(\tau_0) = 0$]. This means the effect of initial random transverse flow is more significant than that of mini-jets propagation in the cur-

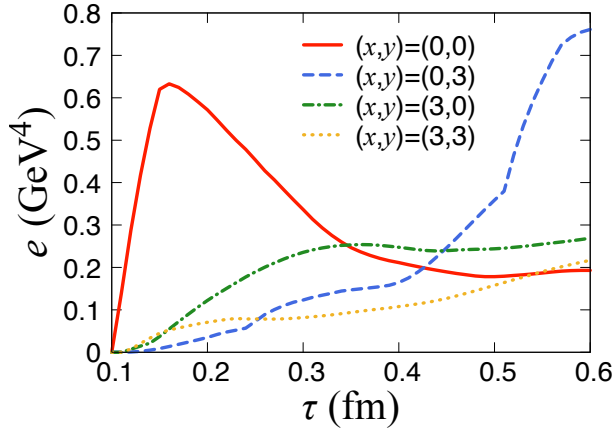


FIG. 3. (Color online) An example of the time evolution of the energy density in units of GeV^4 at four representative transverse positions $(x, y) = (0, 0)$, $(3, 0)$, $(0, 3)$, and $(3, 3)$ fm during dynamical initialization $\tau_{00} < \tau < \tau_0$.

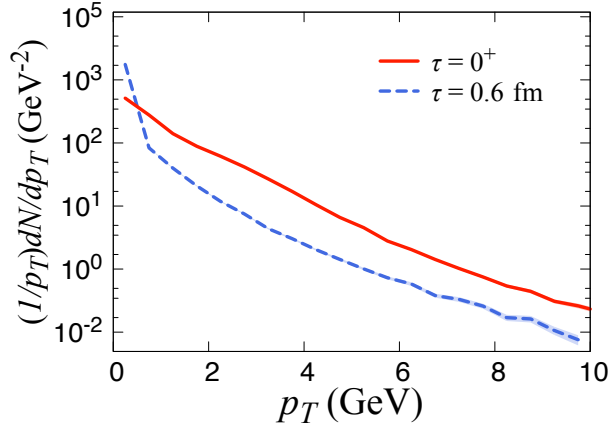


FIG. 4. (Color online) The p_T spectra of the partons at $\tau = 0$ (red solid line) and τ_0 (blue dashed line) in a 30%-40% Pb+Pb collision at $\sqrt{s_{NN}} = 2.76$ TeV. The impact parameter is $b = 9.32$ fm and the number of the event is $N_{ev} = 10^2$.

rent setting.

Shown in Fig. 6 is the elliptic flow coefficient $v_2(p_T)$ of charged pions at midrapidity for different centrality classes with the default setting $[\Delta E \neq 0, v_T(\tau_0) \neq 0]$ in our model. Here one can confirm the increase in v_2 with centrality, which is consistent with hydrodynamic results with conventional initialization. This means that the shape of the participants' region of nuclear collisions still has the largest contribution to v_2 even when there exist additional flow sources other than the initial pressure-gradient profile, i.e., the initial random transverse flow and the mini-jet induced flow. One also sees non-zero v_2 even at "0%" centrality ($b = 0$ fm) caused by the event-by-event fluctuations of the initial profile and flow velocity of the medium.

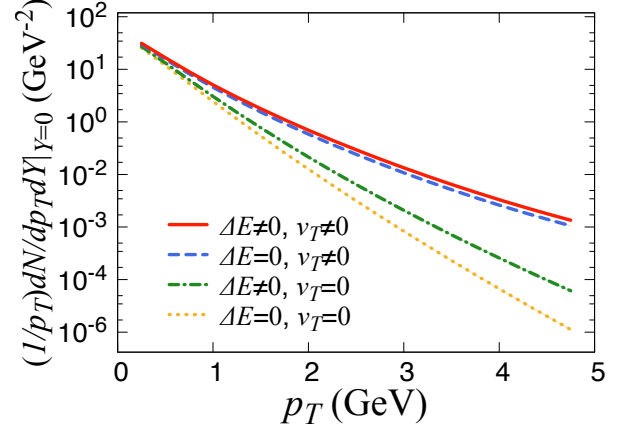


FIG. 5. (Color online) The p_T spectra of charged pions in a 40%-50% Pb+Pb collision at $\sqrt{s_{NN}} = 2.76$ TeV with different settings for the initial flow and for the mini-jets' energy deposition. The impact parameter is $b = 10.58$ fm and the number of the event is $N_{ev} = 10^2$.

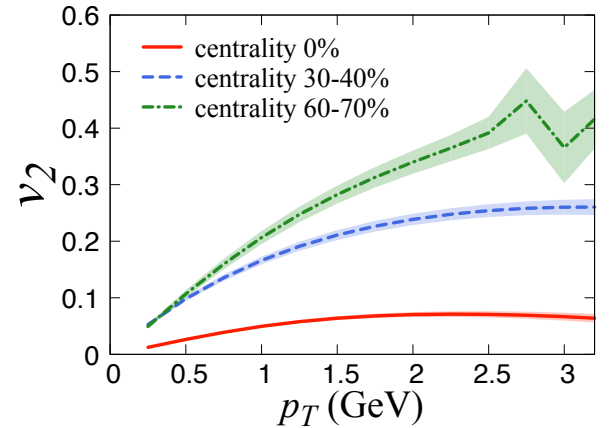


FIG. 6. (Color online) The transverse-momentum dependence of elliptic flow parameter v_2 of the charged pions at midrapidity $Y = 0$ for centrality classes, 0%, 30%-40%, and 60%-70%, in Pb+Pb collisions at $\sqrt{s_{NN}} = 2.76$ TeV.

Figure 7 shows $v_2(p_T)$ of the charged pions at midrapidity in the four different settings in our model. In the low transverse momentum region of $p_T \sim 0-2$ GeV, one sees a little enhancement due to the initial flow fluctuations driven during the dynamical formation of the medium fluid. v_2 at high p_T is dominated by the pions emitted from the medium with large flow velocity at freeze-out. When the initial flow velocity at τ_0 and the mini-jets energy loss are turned off $[\Delta E = 0, v_T(\tau_0) = 0]$, the medium flow velocity in the transverse direction is driven solely by the initial pressure gradient in the medium at τ_0 . In particular, the region with large flow velocity in the medium strongly reflects the initial

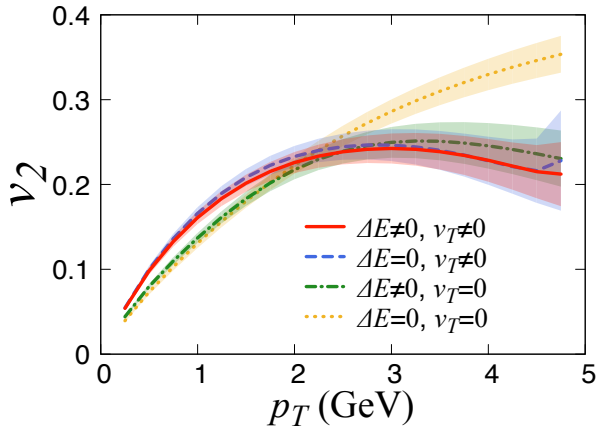


FIG. 7. (Color online) The transverse-momentum dependence of elliptic flow parameter v_2 of the charged pions at midrapidity $Y = 0$ in 40%-50% Pb+Pb collision at $\sqrt{s_{NN}} = 2.76$ TeV, with different settings for the initial flow and for the mini-jets' energy deposition. The impact parameter is $b = 10.58$ fm, and the number of the event is $N_{ev} = 10^2$.

profile of the medium and, as a result, $v_2(p_T)$ monotonically increases. On the other hand, when the initial random transverse flow velocity exists at $\tau = \tau_0$ and/or the mini-jets lose energy and momentum, the large flow velocity in the medium mainly is induced by the momentum deposition through the source term dynamically, and it is not necessary to be aligned with that driven by the initial pressure gradient. As a result, the flow originating from the initial pressure gradient is disturbed and one can no longer see the monotonic increase in $v_2(p_T)$ when there are additional flow sources other than the pressure gradient of the initial profile. Regarding this point, it might be interesting to analyze factorization ratios $r_2(p_T^a, p_T^b)$ [57] for quantitative understanding of event plane decorrelation in the transverse-momentum direction within the current framework.

Figure 8 shows triangular flow coefficient $v_3(p_T)$ of the charged pions at midrapidity in the four different settings in our model. One sees that the initial flow fluctuations driven by the dynamical medium formation largely enhances the triangular flow. Triangular flow is induced mainly by the initial fluctuations, and the global profile of the medium does not affect v_3 significantly. We also find the effect of mini-jet propagation on v_3 is not large.

IV. SUMMARY

In this paper, we formulated a new model to generate the medium evolving hydrodynamically in high-energy nuclear collisions. In the model, all the matters are supposed to be produced from partons created at the first contact of two nuclei. Combining PYTHIA with the MC-Glauber model, we generated these partons from incoher-

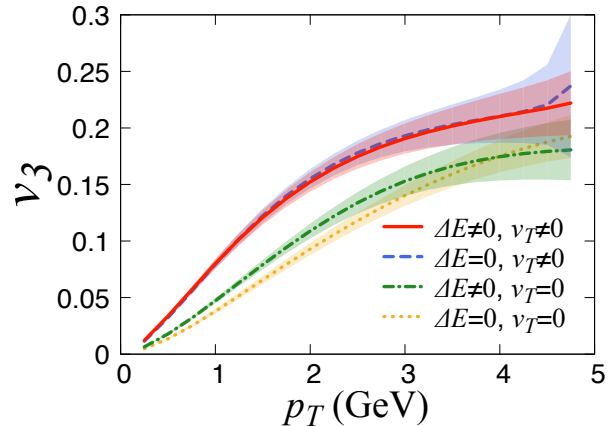


FIG. 8. (Color online) The transverse-momentum dependence of triangular flow parameter v_3 of the charged pions at midrapidity $Y = 0$ in 40%-50% Pb+Pb collision at $\sqrt{s_{NN}} = 2.76$ TeV, with different settings for the initial flow and for the mini-jets' energy deposition. The impact parameter is $b = 10.58$ fm, and the number of the event is $N_{ev} = 10^2$.

ent N_{coll} -times inelastic $p + p$ collisions. Then we applied the rejection sampling to obtain the initial phase-space distribution of the partons which satisfies N_{coll} scaling at high p_T , N_{part} scaling at low p_T , and exhibits rapidity triangle or trapezoid shape in the longitudinal direction at some transverse position. During the propagation through the vacuum after the production, the partons deposit their energy until the hydrodynamic initial time. The deposited energy is used to form the medium fluid dynamically via the source term of hydrodynamic equations. As well as the energy, the momentum also is deposited and, as a result, the medium fluid naturally acquires the initial flow velocity other than that driven purely from the initial pressure gradient. After the hydrodynamic initial time, we regarded the surviving partons as mini-jets traversing the medium fluid. The space-time evolution of the QGP with the energy and momentum deposited by the mini-jets also was described by the hydrodynamic equations with source terms. To obtain the momentum distribution of the charged pions at freeze-out, we employed the Cooper-Frye formula.

First, we saw how the medium and flow velocity are formed during the dynamical generation of the initial hydrodynamic field. The rapid energy-momentum deposition and the expansion of the system compete with each other, and, as a consequence, the energy density of the medium gradually grows. Then we investigated p_T spectra and flow coefficients of azimuthal angle distributions by using the model. In particular we focused on the effects of the initial flow driven during the dynamical formation of the hydrodynamic field and flow induced by the mini-jet propagation. The initial random flow velocity makes the spectrum harder at high p_T . Although the momentum deposition also gives a similar contribution,

it is not so significant.

Next, we investigated the centrality dependence of the elliptic flow coefficient $v_2(p_T)$ in our model. v_2 increases with centrality as the hydrodynamic calculations with conventional initial-condition models, which indicates that the initial global shape of the medium also dominantly affects v_2 in our model. To study how the initial random flow velocity driven during the dynamical initialization and mini-jet induced flow affect anisotropic flow, we calculated $v_2(p_T)$ and $v_3(p_T)$ of the charged pions at midrapidity with different settings for the initial condition. Both the initial random flow velocity and the mini-jet-induced flow disturb the flow driven by the initial pressure gradient and, as a result, suppress v_2 at high p_T . On the other hand, the significant enhancement of v_3 was seen in the case with the the initial random flow velocity. Thus, we found the initial random transverse

flow and the mini-jet induced flow indeed cause sizable anisotropic flow in the QGP fluid. This strongly suggests the conventional hydrodynamic interpretation of flow data based solely on initial eccentricity should be revisited by taking account of the corrections from mini-jet propagation and initial random velocity fields.

ACKNOWLEDGEMENT

The authors are very indebted to H. Hamagaki for fruitful discussions in the very early stage of this study. YT is grateful to Y. Hirono for helpful discussions regarding numerical implementations. YT also acknowledges the kind hospitality of the nuclear theory group at Lawrence Berkeley National Laboratory where parts of this paper were completed.

-
- [1] K. Yagi, T. Hatsuda, and Y. Miake, *Camb. Monogr. Part. Phys. Nucl. Phys. Cosmol.* **23**, 1 (2005).
- [2] K. H. Ackermann *et al.* (STAR), *Phys. Rev. Lett.* **86**, 402 (2001), [arXiv:nucl-ex/0009011 \[nucl-ex\]](#).
- [3] C. Adler *et al.* (STAR), *Phys. Rev. Lett.* **87**, 182301 (2001), [arXiv:nucl-ex/0107003 \[nucl-ex\]](#).
- [4] C. Adler *et al.* (STAR), *Phys. Rev. Lett.* **89**, 132301 (2002), [arXiv:hep-ex/0205072 \[hep-ex\]](#).
- [5] C. Adler *et al.* (STAR), *Phys. Rev.* **C66**, 034904 (2002), [arXiv:nucl-ex/0206001 \[nucl-ex\]](#).
- [6] J. Adams *et al.* (STAR), *Phys. Rev.* **C72**, 014904 (2005), [arXiv:nucl-ex/0409033 \[nucl-ex\]](#).
- [7] K. Adcox *et al.* (PHENIX), *Phys. Rev. Lett.* **89**, 212301 (2002), [arXiv:nucl-ex/0204005 \[nucl-ex\]](#).
- [8] S. S. Adler *et al.* (PHENIX), *Phys. Rev. Lett.* **91**, 182301 (2003), [arXiv:nucl-ex/0305013 \[nucl-ex\]](#).
- [9] B. B. Back *et al.* (PHOBOS), *Phys. Rev. Lett.* **89**, 222301 (2002), [arXiv:nucl-ex/0205021 \[nucl-ex\]](#).
- [10] B. B. Back *et al.* (PHOBOS), *Phys. Rev. Lett.* **94**, 122303 (2005), [arXiv:nucl-ex/0406021 \[nucl-ex\]](#).
- [11] B. B. Back *et al.* (PHOBOS), *Phys. Rev.* **C72**, 051901 (2005), [arXiv:nucl-ex/0407012 \[nucl-ex\]](#).
- [12] P. F. Kolb, P. Huovinen, U. W. Heinz, and H. Heiselberg, *Phys. Lett.* **B500**, 232 (2001), [arXiv:hep-ph/0012137 \[hep-ph\]](#).
- [13] P. F. Kolb, U. W. Heinz, P. Huovinen, K. Eskola, and K. Tuominen, *Nucl. Phys.* **A696**, 197 (2001), [arXiv:hep-ph/0103234 \[hep-ph\]](#).
- [14] D. Teaney, J. Lauret, and E. V. Shuryak, *Phys. Rev. Lett.* **86**, 4783 (2001), [arXiv:nucl-th/0011058 \[nucl-th\]](#).
- [15] T. Hirano, *Phys. Rev.* **C65**, 011901(R) (2001), [arXiv:nucl-th/0108004 \[nucl-th\]](#).
- [16] T. Hirano and K. Tsuda, *Phys. Rev.* **C66**, 054905 (2002), [arXiv:nucl-th/0205043 \[nucl-th\]](#).
- [17] P. Bozek, *Phys. Rev.* **C81**, 034909 (2010), [arXiv:0911.2397 \[nucl-th\]](#).
- [18] H. Song, S. A. Bass, U. Heinz, T. Hirano, and C. Shen, *Phys. Rev. Lett.* **106**, 192301 (2011), [Erratum: *Phys. Rev. Lett.* 109, 139904 (2012)], [arXiv:1011.2783 \[nucl-th\]](#).
- [19] B. Schenke, S. Jeon, and C. Gale, *Phys. Rev. Lett.* **106**, 042301 (2011), [arXiv:1009.3244 \[hep-ph\]](#).
- [20] F. G. Gardim, F. Grassi, M. Luzum, and J.-Y. Ollitrault, *Phys. Rev.* **C85**, 024908 (2012), [arXiv:1111.6538 \[nucl-th\]](#).
- [21] P. Bozek, *Phys. Rev.* **C85**, 034901 (2012), [arXiv:1110.6742 \[nucl-th\]](#).
- [22] Z. Qiu and U. W. Heinz, *Phys. Rev.* **C84**, 024911 (2011), [arXiv:1104.0650 \[nucl-th\]](#).
- [23] Z. Qiu, C. Shen, and U. Heinz, *Phys. Lett.* **B707**, 151 (2012), [arXiv:1110.3033 \[nucl-th\]](#).
- [24] C. Gale, S. Jeon, B. Schenke, P. Tribedy, and R. Venugopalan, *Phys. Rev. Lett.* **110**, 012302 (2013), [arXiv:1209.6330 \[nucl-th\]](#).
- [25] L. Del Zanna, V. Chandra, G. Inghirami, V. Rolando, A. Beraudo, A. De Pace, G. Pagliara, A. Drago, and F. Becattini, *Eur. Phys. J.* **C73**, 2524 (2013), [arXiv:1305.7052 \[nucl-th\]](#).
- [26] H. Niemi, K. J. Eskola, and R. Paatelainen, *Phys. Rev.* **C93**, 024907 (2016), [arXiv:1505.02677 \[hep-ph\]](#).
- [27] L.-G. Pang, H. Petersen, Q. Wang, and X.-N. Wang, *Phys. Rev. Lett.* **117**, 192301 (2016), [arXiv:1605.04024 \[hep-ph\]](#).
- [28] S. Ryu, J. F. Paquet, C. Shen, G. S. Denicol, B. Schenke, S. Jeon, and C. Gale, *Phys. Rev. Lett.* **115**, 132301 (2015), [arXiv:1502.01675 \[nucl-th\]](#).
- [29] G. Denicol, A. Monnai, S. Ryu, and B. Schenke, *Nucl. Phys.* **A956**, 288 (2016), [arXiv:1512.08231 \[nucl-th\]](#).
- [30] I. A. Karpenko, P. Huovinen, H. Petersen, and M. Bleicher, *Phys. Rev.* **C91**, 064901 (2015), [arXiv:1502.01978 \[nucl-th\]](#).
- [31] A. G. Knospe, C. Markert, K. Werner, J. Steinheimer, and M. Bleicher, *Phys. Rev.* **C93**, 014911 (2016), [arXiv:1509.07895 \[nucl-th\]](#).
- [32] K. Murase and T. Hirano, *Nucl. Phys.* **A956**, 276 (2016), [arXiv:1601.02260 \[nucl-th\]](#).
- [33] T. Hirano and Y. Nara, *Phys. Rev.* **C66**, 041901 (2002), [arXiv:hep-ph/0208029 \[hep-ph\]](#).
- [34] T. Hirano and Y. Nara, *Phys. Rev. Lett.* **91**, 082301 (2003), [arXiv:nucl-th/0301042 \[nucl-th\]](#).
- [35] T. Hirano and Y. Nara, *Phys. Rev.* **C69**, 034908 (2004), [arXiv:nucl-th/0307015 \[nucl-th\]](#).

- [36] Y. Tachibana and T. Hirano, *Phys. Rev.* **C90**, 021902 (2014), [arXiv:1402.6469 \[nucl-th\]](#).
- [37] Y. He, T. Luo, X.-N. Wang, and Y. Zhu, *Phys. Rev.* **C91**, 054908 (2015), [arXiv:1503.03313 \[nucl-th\]](#).
- [38] J. Casalderrey-Solana, D. Gulhan, G. Milhano, D. Pablos, and K. Rajagopal, *JHEP* **03**, 135 (2017), [arXiv:1609.05842 \[hep-ph\]](#).
- [39] X.-N. Wang, S.-Y. Wei, and H.-Z. Zhang, (2016), [arXiv:1611.07211 \[hep-ph\]](#).
- [40] V. Khachatryan *et al.* (CMS Collaboration), *JHEP* **11**, 055 (2016), [arXiv:1609.02466 \[nucl-ex\]](#).
- [41] Y. Tachibana, N.-B. Chang, and G.-Y. Qin, *Phys. Rev.* **C95**, 044909 (2017), [arXiv:1701.07951 \[nucl-th\]](#).
- [42] M. Schulc and B. Tomášik, *Phys. Rev.* **C90**, 064910 (2014), [arXiv:1409.6116 \[nucl-th\]](#).
- [43] T. Sjostrand, S. Mrenna, and P. Z. Skands, *Comput. Phys. Commun.* **178**, 852 (2008), [arXiv:0710.3820 \[hep-ph\]](#).
- [44] M. L. Miller, K. Reygers, S. J. Sanders, and P. Steinberg, *Ann. Rev. Nucl. Part. Sci.* **57**, 205 (2007), [arXiv:nucl-ex/0701025 \[nucl-ex\]](#).
- [45] Y. Tachibana and T. Hirano, *Phys. Rev.* **C93**, 054907 (2016), [arXiv:1510.06966 \[nucl-th\]](#).
- [46] F. Cooper and G. Frye, *Phys. Rev.* **D10**, 186 (1974).
- [47] S. J. Brodsky, J. F. Gunion, and J. H. Kuhn, *Phys. Rev. Lett.* **39**, 1120 (1977).
- [48] A. Adil and M. Gyulassy, *Phys. Rev.* **C72**, 034907 (2005), [arXiv:nucl-th/0505004 \[nucl-th\]](#).
- [49] T. Hirano, U. W. Heinz, D. Kharzeev, R. Lacey, and Y. Nara, *Phys. Lett.* **B636**, 299 (2006), [arXiv:nucl-th/0511046 \[nucl-th\]](#).
- [50] T. Hirano, P. Huovinen, K. Murase, and Y. Nara, *Prog. Part. Nucl. Phys.* **70**, 108 (2013), [arXiv:1204.5814 \[nucl-th\]](#).
- [51] K. Kawaguchi, K. Murase, and T. Hirano, *Proceedings, 46th International Symposium on Multiparticle Dynamics (ISMD 2016): Jeju Island, South Korea, EPJ Web Conf.* **141**, 01009 (2017).
- [52] S. Borsanyi, Z. Fodor, C. Hoelbling, S. D. Katz, S. Krieg, and K. K. Szabo, *Phys. Lett.* **B730**, 155 (2014), [arXiv:1312.2193 \[hep-lat\]](#).
- [53] J. D. Bjorken, *Phys. Rev.* **D27**, 140 (1983).
- [54] B. Betz, J. Noronha, G. Torrieri, M. Gyulassy, and D. H. Rischke, *Phys. Rev. Lett.* **105**, 222301 (2010), [arXiv:1005.5461 \[nucl-th\]](#).
- [55] S. Chatrchyan *et al.* (CMS Collaboration), *Eur. Phys. J.* **C72**, 1945 (2012), [arXiv:1202.2554 \[nucl-ex\]](#).
- [56] B. Abelev *et al.* (ALICE Collaboration), *Phys. Lett.* **B720**, 52 (2013), [arXiv:1208.2711 \[hep-ex\]](#).
- [57] F. G. Gardim, F. Grassi, M. Luzum, and J.-Y. Ollitrault, *Phys. Rev.* **C87**, 031901 (2013), [arXiv:1211.0989 \[nucl-th\]](#).